ACS OMEGA

http://pubs.acs.org/journal/acsodf

Article

Improved Harmony Search Algorithm for Enhancing Efficiency and Quality in Optimization of the Distillation Process

Zhe Ding, Haohao Zhang, Hai Li, Jinyi Chen, Ping Lu, and Chao Hua*

Cite This: *ACS Omega* 2023, 8, 28487−28498

Read Online

ACCESS | Metrics & More | Article Recommendations | Supporting Information

ABSTRACT: Reducing production costs is one of the main objectives of process intensification; in this work, production costs of the distillation process are reduced by reducing equipment size and utility consumption from the perspective of process optimization to achieve the purpose of process intensification. The application of intelligent optimization algorithms in the optimization process of distillation is vital to achieving high efficiency and low costs. Combining the harmony search algorithm with the characteristics of distillation optimization, a new distillation harmony search algorithm (DHSA) was proposed, which includes the self-adaptive adjustment of parameters, roulette selection strategy, and ratio optimization strategy. Benefiting from the DHSA, the optimal total annual cost and calculation times were remarkably reduced when compared with reported algorithms in the optimization of four distillation cases including the two-column model, three-column model, reactive distillation column model, and dividing-wall extractive distillation column model. In addition, the highest coefficient of variation of DHSA in 10 parallel calculations is 1.25%. These results indicate that DHSA has the advantages of a higher-quality solution, less computing time, and higher stability, which not only improves the optimization efficiency and quality but also inspires the optimization strategies for other algorithms.

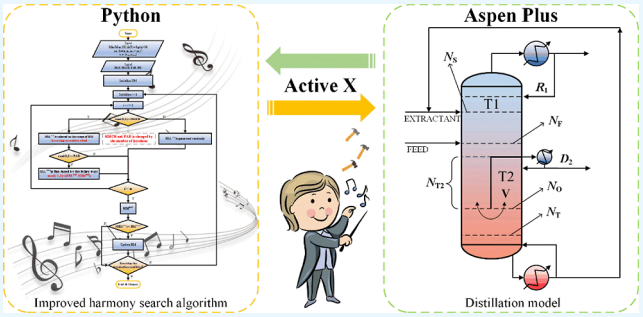

1. INTRODUCTION

With the intensification of competition in the chemical industry and the improvement of design levels, higher requirements are put forward for process design and optimization. Distillation is a commonly used separation method for material separation[1] which utilizes the difference in boiling points of different substances. The mathematical modeling of distillation can be based on the principles of material balance, energy balance, phase equilibrium, and concentration normalization

$$\text{Material balance: } F_i = D_i + W_i$$

$$\text{Energy balance: } Q_F + Q_R = Q_C + Q_D + Q_W$$

$$\text{Phase equilibrium: } y_i = f(x_i)$$

$$\text{Concentration normalization: } \sum x_i = 1;\ \sum y_i = 1$$

In the above equation, F represents the feed, D represents the distillate, and W represents the bottom product. i represents the i-th component. Q_F and Q_R denote the heat input from the feed and reboiler, respectively. Q_C, Q_D, and Q_W represent the heat removal through the condenser, distillate, and bottom product, respectively. x represents the liquid-phase composition, and y represents the vapor-phase composition. By using the above equations, usually combined with inequality constraints specified for the product, a distillation process can be designed. These tasks can be easily performed in simulation software such as Aspen Plus. The strict design and optimization of the distillation process are of great significance for reducing energy consumption, saving costs, and reducing environmental pollution.[2] The distillation process involves multiple decision variables, such as the total stage (N), feed stage (N_F), reflux ratio (R), distillate flow rate (D), pressure (P), and so forth, in which the reflux ratio and pressure are continuous variables and the rest are discrete variables. In addition, product purity (Xp), recovery (R_P), and so forth are often used as constraints and the total annual cost (TAC) is an evaluation index. Therefore, this type of distillation optimization problem can be formulated as a mixed integer nonlinear programming problem (MINP),[3] and it can be described mathematically as follows[4]

$$\text{TAC} = \text{Min}\boldsymbol{f}(N, N_F, R, D, P, \cdot\cdot)$$

Received: April 23, 2023
Accepted: June 28, 2023
Published: July 26, 2023

Subject to: X_p, R_p

The sequential iteration method (SIM) is the earliest and most widely used method to optimize the distillation process. For instance, Hosgor et al.[5] optimized a methanol/chloroform system by using the SIM, and Geng et al.[6] optimized a methyl acetate hydrolysis reaction in a dividing-wall column by utilizing the strategy of the SIM. The SIM searches for the minimum value of TAC by gradually changing variables one by one, but the optimization of one variable is limited by other fixed variables. Although the SIM can achieve the purpose of optimization, it usually provides poor quality results even after costing a long calculation time.

To make distillation process optimization more efficient, some intelligent optimization algorithms have been applied to the optimization process. The simulated annealing algorithm[7] was originally motivated by the process of physical annealing in metalwork and successfully applied in distillation optimization.[8−11] The genetic algorithm (GA)[12] is an intelligent optimization algorithm to search for the global optimal solution by simulating the natural evolution process; research shows that if the GA can be used correctly, it will solve the optimization problem more efficiently.[2,13−15] The particle swarm optimization algorithm (PSOA)[16] is an evolutionary algorithm developed by simulating the foraging behavior of gregarious organisms, and it has been used to complete optimization tasks.[16−18]

The successful application of these algorithms shows the feasibility of intelligent optimization algorithms in chemical process optimization; thus, using different algorithms in chemical process optimization has gradually been a research highlight. With the rapid development of intelligent optimization algorithms, different algorithms have been developed to improve efficiency. The harmony search algorithm (HSA)[19] has been developed by simulating the performance behavior of musicians by repeatedly adjusting the size of different tones in the harmony. It has several advantages such as all solutions having a chance to influence the generation of new solutions, the value of each dimension of the new solution being generated independently, and a noncontinuous variable being permitted. The difference between the HSA and other intelligent optimization algorithms is shown in Figure 1 (the darker dot is closer to the optimal solution); the difference is mainly reflected in the update

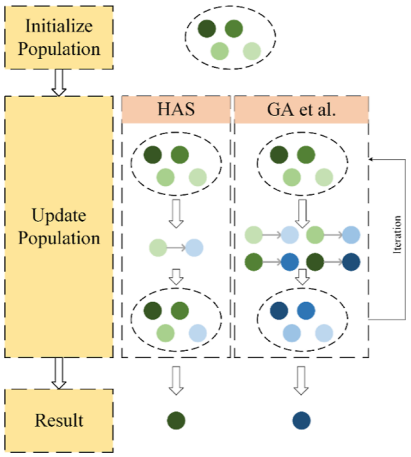

Figure 1. Process of intelligent optimization algorithms.

population; stage HSA updates only one solution in the population in each iteration process, while the GA and PSOA require computing each solution in the population to form a new population. Due to the HSA's characteristics, it can improve the optimization efficiency by avoiding unreasonable updates in the calculation process and transferring the optimal value to the next iteration. Therefore, the HSA is widely concerned in various optimization problems for its excellent scalability and fast solution speed, such as mathematical problems,[20] assembly variations,[21] special truss structures,[22] object detection,[23] economic dispatch,[24] vehicle routing,[25] buffer allocation problem,[26] and tool indexing.[27] However, the HSA will fall into the trap of local optimal solution inevitably according to the small amount of calculation. Thus, it is of great significance to optimize the HSA to enhance the optimization efficiency by improving the global search ability and giving play to its advantage of less calculation time.

Based on the classical HSA, this work combined the characteristics of distillation process optimization and developed a universal distillation process optimization algorithm (DHSA) by using Python and Aspen Plus. The application of the SIM, GA, PSOA, and DHSA in four distillation process optimization models was discussed. In addition, the difference of the DHSA in 10 parallel optimization results was analyzed. The calculation results showed that the improved DHSA has excellent optimization ability and stability, which is suitable for the optimization of the distillation process.

2. IMPROVEMENTS OF THE HSA

Assume that $f(x)$ is the objective function and the HSA is used to search the minimum value in the range [L, U], where L and U represent the lower and upper bounds of the search domain, respectively. The steps of the HSA are as follows, and the flowchart is shown in Figure 2 (without the red part):

(1) Initialize the parameters. The classical HSA has four main control parameters,[19] including harmony memory size (HMS), harmony memory considering rate (HMCR), pitch adjusting rate (PAR), and bandwidth (BW).

(2) Initialize the HM. As shown in Formula 1, HMS harmonies are generated to form HM randomly.

$$\mathrm{HM}_{i,j} = L_j + (U_j - L_j) \times \mathrm{rand}(-1,1)$$

where $x_{i,j}$ is the j-th dimension of the i-th harmony.

(3) Improvisation. Generate a new harmony according to HM's strategy. The pseudocode is shown below.

```
for j in range(1,HMS):
    if rand(0,1) < HMCR:
        HM_new,j = HM_i,j , i∈[1,2,....,HMS]
        if rand(0,1) < PAR:
            x_new,j = x_new,j + rand(−1,1) × bw
    else:
        HM_new,j = L_j + (U_j − L_j) × rand(0,1)
if f(HM_new) < f(HM_worst) :
    HM_worst = HM_new
```

(4) Go to step (2) until the stopping criteria are met.

To improve the performance of HSA and better match the distillation optimization work, we proposed some improvement measures for this algorithm.

https://doi.org/10.1021/acsomega.3c02785
ACS Omega 2023, 8, 28487−28498

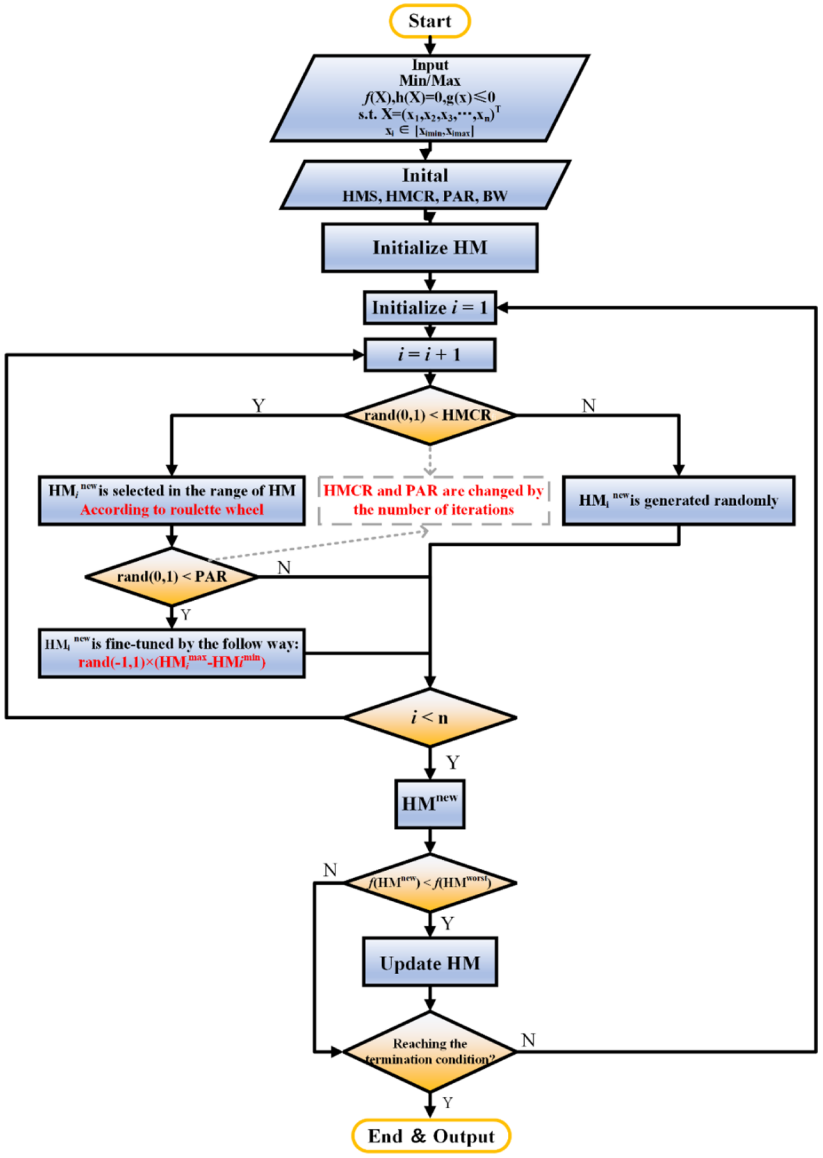

Figure 2. Flowchart of the HSA and DHSA.

2.1. Self-Adaptive HMCR and PAR. It is clearly explained by the developers of the HSA for the role of these parameters that the HMCR supports the large-scale exploration and PAR helps in further exploiting.[19] Thus, reasonable HMCR and PAR are crucial and responsible for controlling the HSA to achieve better results. The fixed parameter set in classical HSA limits its optimization ability; Kumar et al.[28] have modified the search strategy of the HSA by introducing Formulas 1−4 owing to HMCR and PAR; they can keep linearly and nonlinearly changing during the search process.

$$\mathrm{HMCR}_t^{\mathrm{linear}} = \mathrm{HMCR}^{\min} + (t/T^{\max})(\mathrm{HMCR}^{\max} - \mathrm{HMCR}^{\min}) \quad (1)$$

$$\mathrm{HMCR}_t^{\text{non-linear}} = \mathrm{HMCR}^{\min}\exp\left(-t/\mathrm{T}^{\max}\ln\left(\frac{\mathrm{HMCR}^{\min}}{\mathrm{HMCR}^{\max}}\right)\right) \quad (2)$$

$$\mathrm{PAR}_t^{\mathrm{linear}} = \mathrm{PAR}^{\min} + t/\mathrm{T}^{\max}(\mathrm{PAR}^{\max} - \mathrm{PAR}^{\min}) \quad (3)$$

$$\mathrm{HMCR}_t^{\text{non-linear}} = \mathrm{HMCR}^{\min}\exp\left(-t/\mathrm{T}^{\max}\ln\left(\frac{\mathrm{HMCR}^{\min}}{\mathrm{HMCR}^{\max}}\right)\right) \quad (4)$$

where t indicates the current iteration and $T^{\max}$ is the maximum number of iterations. $\mathrm{HMCR}^{\min}$ and $\mathrm{HMCR}^{\max}$ are the minimum and maximum values of HMCR, respectively, which can also be defined as starting and ending values. $\mathrm{PAR}^{\min}$ and $\mathrm{PAR}^{\max}$ have the same meaning as $\mathrm{HMCR}^{\min}$ and $\mathrm{HMCR}^{\max}$. In addition to the above improvement measures, there are some researchers who have tried to reveal how the HMCR and PAR affect the ability of the has;[29−31] these works have proved that during the optimization process, a smaller HMCR and PAR at the initial phase and a larger HMCR and PAR at the final phase are conducive to increase the efficiency of the HSA. To make the HMCR and PAR play a better role in regulating the algorithm capability, this work proposes the self-adaptive control strategies as Formulas 5 and 6.

https://doi.org/10.1021/acsomega.3c02785
ACS Omega 2023, 8, 28487−28498

$$\mathrm{HMCR}_t = \mathrm{HMCR}^{\min} + (\mathrm{HMCR}^{\max} - \mathrm{HMCR}^{\min}) \left(\frac{1}{1 + e^{-7+15\times t/\mathrm{T}^{\max}}}\right) \quad (5)$$

$$\mathrm{PAR}_t = \mathrm{PAR}^{\min} + (\mathrm{PAR}^{\max} - \mathrm{PAR}^{\min}) \left(\frac{1}{1 + e^{-7+15\times t/\mathrm{T}^{\max}}}\right) \quad (6)$$

Here, HMCR_t and PAR_t are the values of the t-th iteration, and they gradually increase as the iteration progresses. The change trend corresponding to the formula is shown in Figure 3. The HMCR and PAR can hold smaller values at the initial phase and larger values at the final phase compared with other strategies; therefore, they can play a better role in regulating the algorithm.

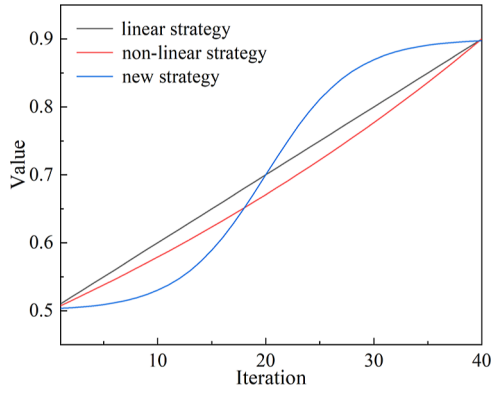

Figure 3. Trend of different strategies.

2.2. Harmony Selection Strategy. In the classical HSA, the i-th component of $\mathrm{HM}^{\mathrm{new}}$ ($\mathrm{HM}_i^{\mathrm{new}}$) will be selected randomly from HM; it will lead to slow convergence due to the aimless optimization. Therefore, it is necessary to propose an effective selection strategy; Jaberipour and Khorram[32] select the $\mathrm{HM}_i^{\mathrm{new}}$ from the worst harmony ($\mathrm{HM}_i^{\mathrm{worst}}$) in the current HM; Guo et al.[33] select the $\mathrm{HM}_i^{\mathrm{new}}$ from the best harmony $\mathrm{HM}_i^{\mathrm{best}}$ in the current HM; these methods show good performance in respective problems. In the process of distillation optimization, designers consider that the current optimal solution is closer to the global optimal solution than other solutions in most cases; thus, optimizing the current optimal solution will help designers find the global optimal solution quickly. However, due to the characteristics of the MINP problem, the poorer solutions also can converge to the global solution to a certain degree. Based on the above analysis, this work proposes a roulette selection strategy; when selecting an $\mathrm{HM}_i^{\mathrm{new}}$, the current optimal solution with a large probability is selected and it is ensured that there also is a certain probability to choose other solutions. Figure 4 shows the roulette selection strategy; the values of A to F are 30, 20, 20, 15, 10, and 5, respectively, with the maximum value being the optimization goal; the fitness of A can be calculated as 0.3 [30/(30 + 20 + 20 + 15 + 15 + 5)]; thus, A is selected with a probability of 30%.

In the optimization of the distillation process, the lower TAC is desirable, so the TAC cannot be directly regarded as fitness; it will bring the opposite result. For this reason, the relationship between the TAC and fitness should be established. TAC_j is the calculated result of the solution HM_j in HM, and $\mathrm{TAC}_{\max}$ is the calculated result of the worst solution $\mathrm{HM}^{\mathrm{worst}}$. The fitness of different solution FIT_j is calculated by Formulas 7 and 8

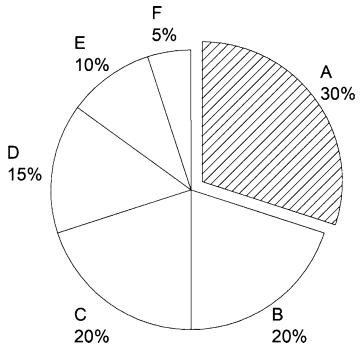

Figure 4. Schematic diagram of the roulette selection strategy.

$$\mathrm{FIT}_j = \mathrm{TAC}_j - \mathrm{TAC}_{\max} \quad (7)$$

$$P_j = \frac{\mathrm{FIT}_j}{\sum_{i=1}^{\mathrm{HSM}} \mathrm{FIT}_i} \quad (8)$$

where P_j is the selection probability of HM_j; from this strategy, the HM_j corresponding to the lower TAC has a greater selection probability.

2.3. Self-Adaptive BW. BW is set during initialization in HSA; it influences the fine-tuning of new harmony through Formula 9

$$\mathrm{HM}_i^{\mathrm{new}} = \mathrm{HM}_i^{\mathrm{new}} + \mathrm{rand}(-1,1) \times \mathrm{BW} \quad (9)$$

At the beginning of the calculation, the larger BW can increase the diversity of HM; with the calculation going on, the solutions in HM are closer, and the larger BW will cause $\mathrm{HM}^{\mathrm{new}}$ to skip the optimal solution. Therefore, dynamic adjustment of the BW is also an important way to optimize HSA. Chakraborty et al.[34] have adopted a mutation method, which is applied in the DE algorithm; the new harmony is fine-tuned by Formula 10

$$\mathrm{HM}_i^{\mathrm{new}} = \mathrm{HM}_i^{\mathrm{new}} + \mathrm{rand}(-1,1) \times (\mathrm{HM}_i^{\mathrm{rand1}} - \mathrm{HM}_i^{\mathrm{rand2}}) \quad (10)$$

where $\mathrm{HM}_i^{\mathrm{rand1}}$ and $\mathrm{HM}_i^{\mathrm{rand2}}$ are the i-th components of the randomly selected and different harmonies from the current HM. Although this tactic can increase exploration ability, it will bring about a standstill and long-time oscillation. Jaberipour and Khorram[32] have utilized the global best and worst harmony to improve the ability of the HSA through Formulas 10 and 11

$$\mathrm{HM}_i^{\mathrm{new}} = \mathrm{HM}_i^{\mathrm{new}} + \mathrm{rand}(-1,1) \times (\mathrm{HM}_i^{\mathrm{R}} - \mathrm{HM}_i^{\mathrm{worst}}) \quad (11)$$

$$\mathrm{HM}_i^{\mathrm{R}} = (2\mathrm{HM}_i^{\mathrm{best}} - \mathrm{HM}_i^{\mathrm{worst}}) \quad (12)$$

In the MINP problem, the discrete variable, such as the total stage, will have the same value in different harmonies, even the worst harmony and the best harmony; it causes the BW to be zero by using the above strategies, resulting in a loss of regulatory effects. For this reason, it is necessary to propose a strategy that can solve the influence of discrete variables. Considering that the maximum and minimum values of the i-th

https://doi.org/10.1021/acsomega.3c02785
ACS Omega 2023, 8, 28487−28498

component in HM are always different; this work adopted Formula 13 to update BW in each iteration

$$HM_i^{new} = HM_i^{new} + rand(-1,1) \times (HM_i^{max} - HM_i^{min}) \quad (13)$$

As optimization proceeds, the difference between HM_i^{max} and HM_i^{min} gets smaller; it realizes the self-adaptive adjustment of the BW.

2.4. Decision Variable. In general, the feed stage and the stage of the section in the distillation column are decision variables; they are often optimized individually. However, according to the design experience that both of them are related to the total stage, for example, the feed stage generally increases with the increase of the total stage. To take this relationship into account in the optimization, the ratio of the feed stage and the stage of the section in the distillation column to the total stage was used as a decision variable in this work. The fraction form was utilized for data analysis and valuation in the algorithm, and the integer form was utilized for calculating it in process simulation, so it realized the connection between fractions and integers.

The DHSA is proposed by all the above improvement measures, and the optimized flowchart is shown in Figure 2 (with the red part).

3. METHODS OF DISTILLATION OPTIMIZATION

The realization of distillation process optimization is shown in Figure 5; codes of algorithms were written based on Python

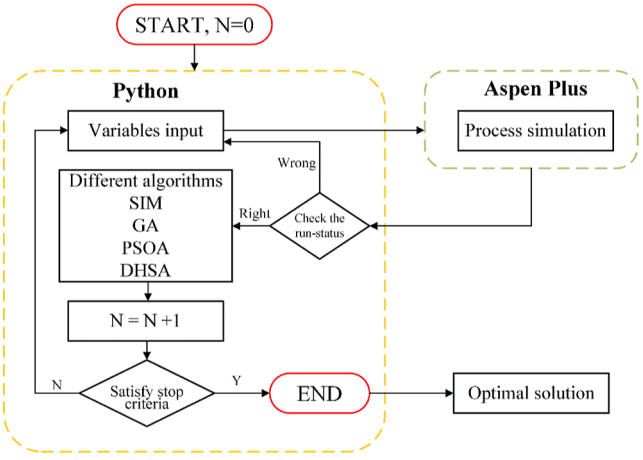

Figure 5. Distillation process optimization by using Python and Aspen Plus.

(V3.9) (the main code is listed in the first part of the Supporting Information). Aspen Plus (V9.0) was used to simulate the distillation process, and Python was used to call the Aspen Plus (V9.0) interface to implement data input, operation, extraction, and other operations. Data processing and process optimization using different algorithms were carried out in Python.

The workflow is as follows:

(1) Establishing a distillation process in Aspen Plus which should be completed without errors on selected initial parameters;

(2) Determining the decision variables and using the "Design-spec/Vary" (DV) function of Aspen Plus to satisfy the constraints by automatically adjusting specific variables so that it can reduce the number of variables. The rough search space can be determined by analyzing the relationship between results and variables using the "Sensitivity Analysis" (SA) function of Aspen Plus;

(3) Establishing evaluation function and fitness function. For the distillation process, TAC is used as the objective function which is composed of the total capital cost (TCC) and total operating cost (TOC). The calculation formula is shown as follows:

$$TAC = TCC/\text{payback period} + TOC \quad (14)$$

$$TCC = 17640 \times D^{1.066} \times L^{0.802} + 7296 \times A_C^{0.65} + 7296 \times A_R^{0.65} \quad (15)$$

$$TCC = Q_R \times 8000 \times 3600 \times C_R + Q_C \times 8000 \times 3600 \times C_C \quad (16)$$

where the payback period was equal to 3, D and L represent the diameter and height of the distillation column, A_C and A_R represent the heat transfer area of the condenser and reboiler, and C_C and C_R represent the unit cost cooling water and steam, respectively; all the above were referred from a book.[35]

The fitness function is described in Section 2.2;

(4) The SIM, GA, PSOA, and DHSA (GA, PSOA, and DHSA are intelligent algorithms) were, respectively, used to optimize different distillation process models. Whether the number of optimization calculations reaches the set value or the obtained optimal TAC is steady is judged to stop the optimization. According to the work of Wang et al.,[36] PSOA's population size was equal to 20, the maximum iteration was equal to 20, the inertia weight was equal to 1, and the individual and global learning coefficients were equal to 2. GA's population size was equal to 20, the maximum iteration was equal to 20, the DNA size was equal to 24, the crossover rate was equal to 0.8, and the mutation rate was equal to 0.005 according to Sulgan et al.[37] The initial parameters of the DHSA are shown in Table 1.

Table 1. Initial Parameters of the DHSA

parameter	value
HMS	20
T^{max}	200
$HMCR^{min}$	0.5
$HMCR^{max}$	0.95
PAR^{min}	0.5
PAR^{max}	0.95

It should be noted that the main purpose of this work was to propose a more efficient algorithm; therefore, the four reported distillation process models were adopted and used the same process conditions and design regulations. To compare the optimization results of different algorithms more convincingly, each algorithm was optimized 10 times and the best one was selected (all results are shown in the Supporting Information). The coefficient of variation (CV) was used to evaluate the stability of the optimization algorithm, which is the ratio of the standard deviation to the average value. The size of data

https://doi.org/10.1021/acsomega.3c02785
ACS Omega 2023, 8, 28487−28498

dispersion can be evaluated while eliminating the impact of the original data scale by CV.

4. RESULTS AND DISCUSSION

In this paper, representative process flows including two-column, three-column, reactive distillation, and dividing-wall extractive distillation were selected based on common distillation process configurations. To ensure better reproducibility of the simulation results and facilitate comparison with the literature, the composition, flow rate, temperature, and other process parameters for each different process flow were kept consistent with the reference literature.

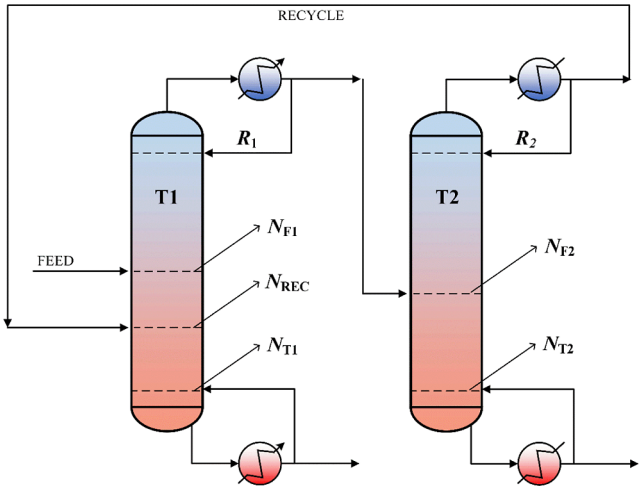

Figure 6. Flow sheet and design variables of case 1.

Table 2. Feed Composition and Design Regulations of Case 1

item	value
feed flow rate (kmol/h)	540
mole fraction of MeOH	0.5
mole fraction of AC	0.5
Design Regulations (mol %)	
MeOH	99.6
AC	99.4

4.1. Case 1: Acetone/Methanol Separation (Two-Column Model). Methanol (MeOH) and acetone (AC) will form an azeotropic system. Luyben et al.[38] have developed a steady-state flowsheet for separating the acetone/methanol mixture using the UNIQUAC thermodynamic method. As shown in Figure 6, this flowsheet includes a lower-pressure column (T1, 0.1 MPa) and a higher-pressure column (T2, 1 MPa). Feed composition and design regulations are shown in Table 2.

The DV was used to guarantee product specifications by changing the product flow rate at the bottom of T1 and T2; then, the decision variables of the process were the total stage of T1 (N_{T1}), the feed stage (N_{F1}), the recycle stream stage (N_{REC}) of T1, the reflux ratio of T1 (R_1), the total stage (N_{T2}) of T2, the feed stage of T2 (N_{F2}), and the reflux ratio of T2 (R_2), and in the DHSA, the ratio of N_{F1} and N_{REC} to N_{T1} and the ratio of N_{F2} to N_{T2} were the decision variables. All design variables are marked in Figure 6. Table 3 shows the range of design variables by using the SA.

The optimization results are shown in Table 3. The optimal TAC obtained by DHSA is 5,590,265 $/y, which is 0.5, 0.9, and 0.6% lower than that of SIM, GA, and PSOA, respectively. In terms of calculation times, DHSA calculated 220 times, and GA and PSOA reached the calculation termination conditions by using 340 and 320 times, respectively. Figure 7a shows the TOC and TCC in different algorithms; it appears that the TOC and TCC did not undergo significant changes, while TOC maintains a relatively high proportion in the TAC. Figure 7b shows 10 optimized results; the optimal TAC is 5,601,787 $/y on average, and the CV is 0.17%. Figure 7c shows the optimization process corresponding to the optimal solution obtained by DHSA in Table 3. The optimal TAC decreases continuously as the calculation proceeds until it reaches the maximum number of calculations.

4.2. Case 2: Silicon Tetrachloride/trichlorosilane/dichlorosilane Separation (Three-Column Model). Trichlorosilane (TCS) purification from the silicon tetrachloride (STC)-TCS-dichlorosilane (DCS) system is an important part of the polysilicon manufacturing process. The TCS distillation steady-state process was simulated using the NRTL thermodynamic method according to Yin et al.,[39] including light-removing column T1, heavy-removing column T2, and product-column T3 (Figure 8). Feed composition and design regulations are shown in Table 4.

Since the product purity is specified, it is worth fixing the product flow rate of T1, T2, and T3 to ensure the recovery rate for less blindness optimization.[39] The DV was used to guarantee product specifications by changing the reflux ratios of T1, T2, and T3. Then, the same decision variables were determined as per a referenced work: the total stage of T1, T2, and T3 (N_{T1}, N_{T2}, and N_{T3}), the feed stage (N_{F1}, N_{F2}, and N_{F3}), and the recycle stream stage (N_{REC}). The ratio of N_{F1} and N_{REC} to N_{T1}, the ratio of N_{F2} to N_{T2}, and the ratio of N_{F3}

Table 3. Variable Range and Optimization Results of Case 1

item	range	SIM	GA	PSOA	DHSA
N_{T1}	[20, 70]	55	69	54	51
N_{T2}	[20, 70]	61	55	67	58
N_{F1}	[2, N_{T1}]	35	48	36	34(0.661)[b]
NREC	[2, N_{T1}]	44	61	47	38(0.750)[b]
N_{F2}	[2, NT_2]	36	33	37	39(0.673)[b]
$R1$	[1, 5]	1.96	1.92	1.85	1.97
$R2$	[1, 5]	3.055569	3.10	2.94	3.00
TAC ($/y)		5,619,943	5,643,184	5,622,595	5,590,265
NAC[a]		700	340	320	220

[a]Number of algorithm calculations. [b]The result is a ratio converted to an integer.

https://doi.org/10.1021/acsomega.3c02785
ACS Omega 2023, 8, 28487−28498

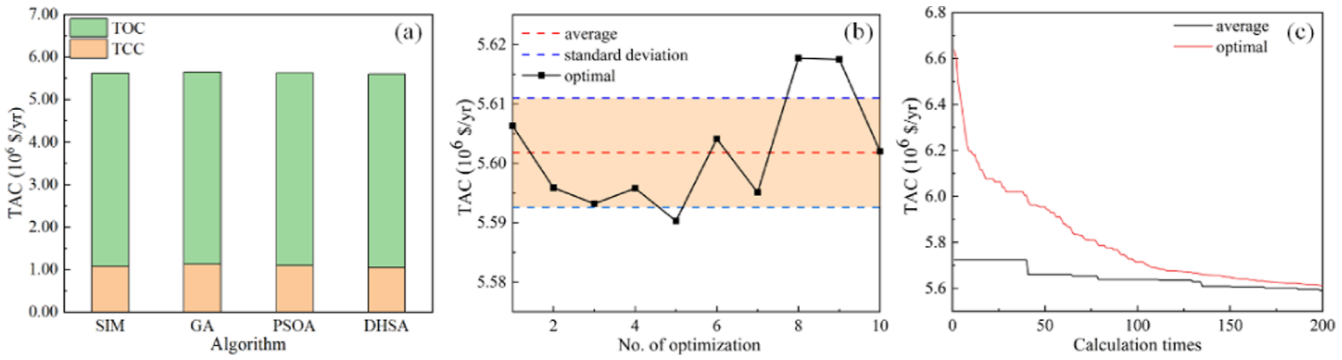

Figure 7. Results of optimization of case 1. TOC and TCC in different algorithms (a); 10 optimization results (b); optimization process (c).

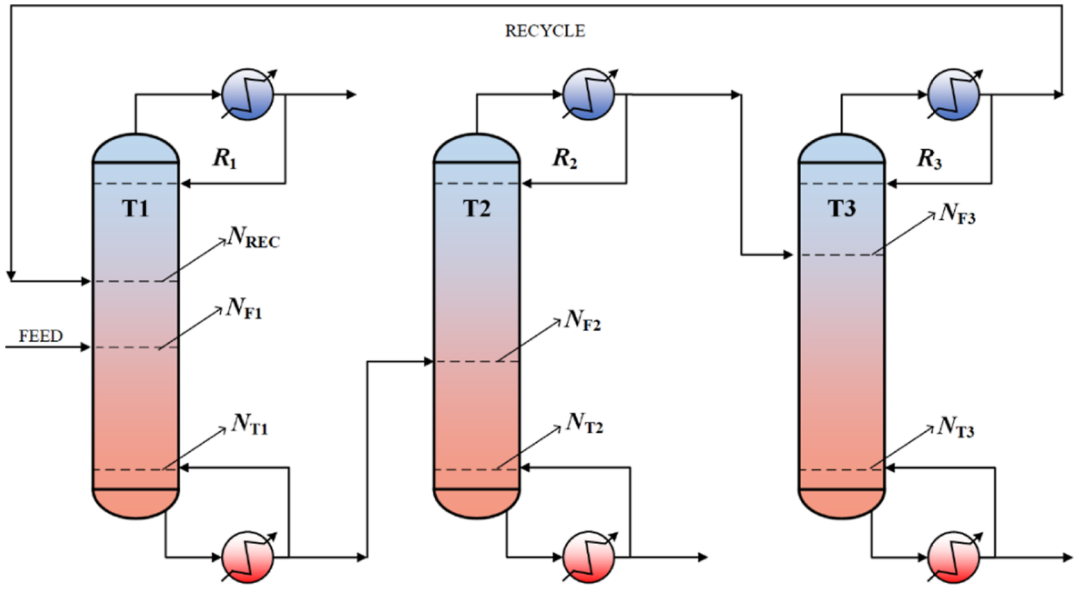

Figure 8. Flow sheet and design variables of case 2.

Table 4. Feed Composition and Design Regulations of Case 2

item	value
feed flow rate (kg/h)	40,000
mass fraction of STC	0.04
mass fraction of TCS	0.92
mass fraction of DCS	0.02
Design Regulations (wt %)	
STC	99.9
TCS	99.99
DCS	99.8

to N_{T3} were decision variables in DHSA. All design variables are marked in Figure 8. Table 5 shows the range of design variables by using SA.

The optimization results are shown in Table 5. The optimal TAC obtained by the DHSA is 2,764,088 $/y, which is 4.2, 3.0, and 1.3% lower than that of the SIM, GA, and POSA respectively. In terms of calculation times, the DHSA reaches the max calculation times, and GA and PSOA stop optimization in advance by 380 and 400. As shown in Figure 9a, the TOC is significantly larger than TCC and the reduction in TAC mainly stems from the decrease in TOC. However, it is important to note that DHSA achieves the lowest TAC, but

Table 5. Variable Range and Optimization Results of Case 2

item	range	SIM	GA	PSOA	DHSA
N_{T1}	[30, 80]	58	56	55	53
N_{T2}	[30, 80]	48	60	58	64
N_{T3}	[30, 80]	61	58	60	62
N_{REC}	[2, N_{T1}]	16	15	12	11(0.211)
N_{F1}	[2, N_{T1}]	25	27	25	28(0.525)
N_{F2}	[2, N_{T2}]	32	43	43	44(0.694)
N_{F3}	[2, N_{T3}]	12	11	10	11(0.182)
TAC ($/y)		2,886,623	2,850,984	2,799,495	2,764,088
NAC		700	380	400	220

https://doi.org/10.1021/acsomega.3c02785
ACS Omega 2023, 8, 28487−28498

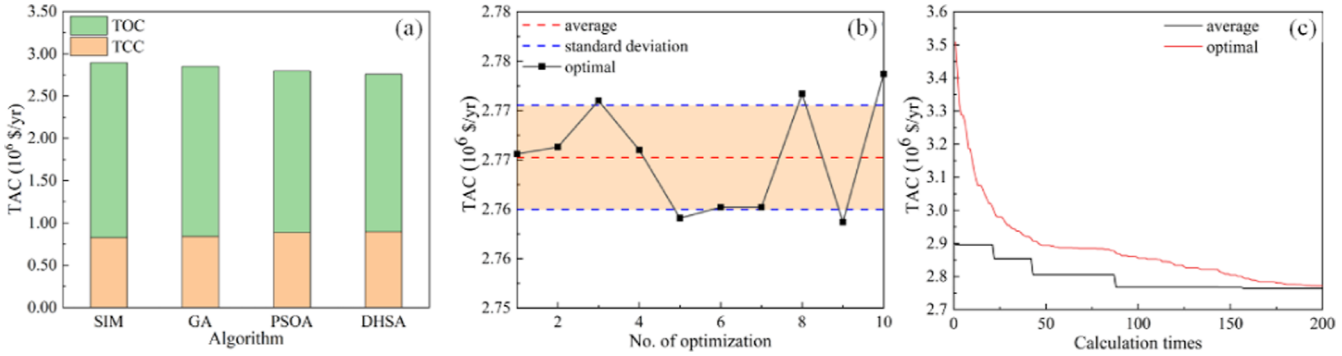

Figure 9. Results of optimization of case 2 TOC and TCC in different algorithms (a); 10 optimization results (b); optimization process (c).

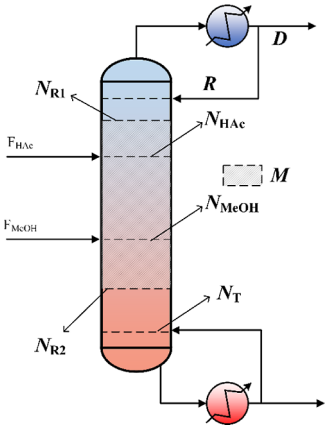

Figure 10. Flow sheet and design variables of case 3.

Table 6. Feed Composition and Design Regulations of Case 3

item	value
feed flow rate (kmol/h)	100
mole fraction of HAc	0.5
mole fraction of MeOH	0.5
Design Regulations (mol %)	
MeAc	98.0
H_2O	98.0

it is associated with a certain degree of increase in TCC. As shown in Figure 9b, the optimal TAC obtained by repeating the DHSA 10 times is 2,770,241 $/y on average, and the CV is 0.19%, close to case 1. Figure 9c shows the optimization process corresponding to the optimal solution obtained by DHSA in Table 5. The optimal TAC decreases continuously as the calculation proceeds until it reaches the maximum number of calculations.

4.3. Case 3: Methyl Acetate Separation (Reactive Distillation Model). Separation of methyl acetate (MeAc) is a typical reactive distillation; the esterification of acetic acid (HAc) with methanol (MeOH) forms MeAc

$$\mathrm{HAc} + \mathrm{MeOH} \rightarrow \mathrm{MeAc} + \mathrm{H_2O} \tag{17}$$

with reference to the work of Huang et al.,[40] the process was established as Figure 10 using the UNIQUAC thermodynamic method. The net reaction rate is expressed by the pseudohomogeneous activity-kinetic model as follows

$$\mathrm{Rate} = M(k_f \alpha_{\mathrm{HAc}} \alpha_{\mathrm{MeOH}} - k_b \alpha_{\mathrm{MeAc}} \alpha_{\mathrm{H_2O}}) \tag{18}$$

$$k_f = 2.914 \times 10^4 \exp(-49.19/RT) \tag{19}$$

$$k_f = 1.348 \times 10^6 \exp(-69.23/RT) \tag{20}$$

Feed composition and design regulations are shown in Table 6.

The DV was used to guarantee product specifications by changing the reflux ratio and extraction of the column top. Then, the decision variables were determined as follows: the total stage (N_T), the feed stage of MeOH and HAc (N_{MeOH} and N_{Hac}, respectively), the start and end stage of the reaction section (N_{R1} and N_{R2}, respectively), and the liquid holdup (M). The ratios of N_{MeOH}, N_{HAc}, N_{R1}, and N_{R2} to N_T were decision variables in the DHSA. All design variables are marked in Figure 10. Table 7 shows the range of design variables by using SA.

The optimization results are shown in Table 7. The optimal TAC obtained by the DHSA is 199,559 $/y, which is 13.1, 7.6, and 5.8% lower than that of the SIM, GA, and POSA respectively. In terms of calculation times, the DHSA stops optimization in advance and less than other algorithms significantly. From Figure 11a, the proportions of the TOC and TCC are similar, and the reduction in the TAC primarily stems from the decrease in the TCC. As shown in Figure 11b,

Table 7. Variable Range and Optimization Results of Case 3

item	range	SIM	GA	PSOA	DHSA
N_T	[20, 70]	39	34	30	26
N_{MeOH}	[2, N_T]	28	18	16	15(0.577)
N_{HAc}	[2, N_T]	7	8	5	6(0.231)
N_{R1}	[2, N_T]	3	11	4	2(0.077)
N_{R2}	[2, N_T]	36	30	21	19(0.731)
M	[0.05, 0.20]	0.18	0.123	0.096	0.187
TAC ($/y)		229,664	216,082	211,828	199,559
NAC		600	420	420	180

https://doi.org/10.1021/acsomega.3c02785
ACS Omega 2023, 8, 28487−28498

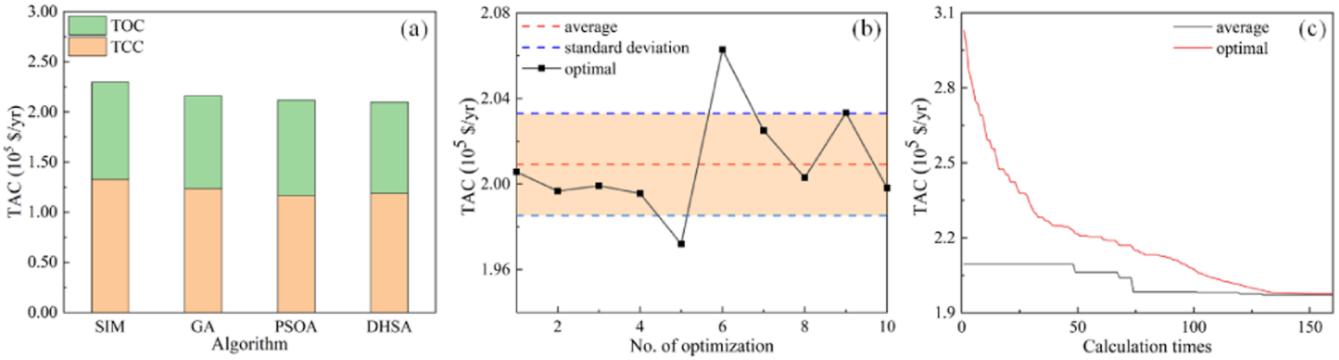

Figure 11. Results of optimization of case 3 TOC and TCC in different algorithms (a); 10 optimization results (b); optimization process (c).

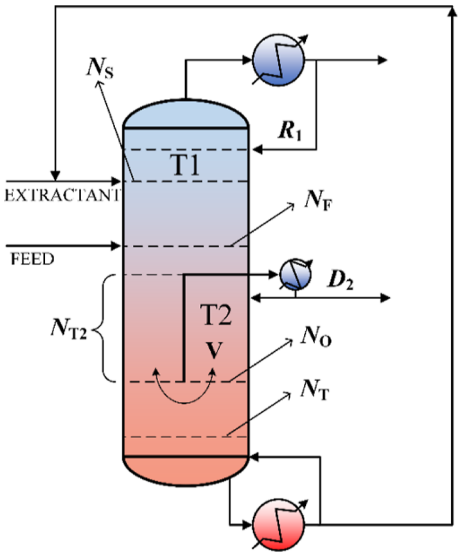

Figure 12. Flow sheet and design variables of case 4.

Table 8. Feed Composition and Design Regulations of Case 4

item	value
feed flow rate (kg/h)	4000
mass fraction of MECN	0.5
mass fraction of N-pro	0.5
Design Regulations (wt %)	
MECN	99.6
N-pro	99.6
NMP	99.97

the optimal TAC obtained by repeating the DHSA 10 times is 200,914 $/y on average, and the CV is 1.25%. Figure 11c shows the optimization process corresponding to the optimal solution obtained by DHSA in Table 7. During the optimization process, the optimal value and average value of the HM keep decreasing. When the number of calculations reaches 180, the optimization stops.

4.4. Case 4: Acetonitrile/N-Propanol Separation (Dividing-Wall Extractive Distillation Model). Acetonitrile (MeCN)/N-propanol (N-Pro) is an azeotropic system. Tian[41] has designed a dividing-wall extractive distillation process by using *N*-methyl pyrrolidone (NMP) as an extractant and employing the Wilson-RK thermodynamic method. There are two columns shown in Figure 12; one is the main column (T1) and the other is the auxiliary column (T2). Feed composition and design regulations are shown in Table 8.

The DV was used to guarantee product specifications by changing the reflux ratios of T1 and extraction of T2. To meet the NMP purity requirement, Python was used to judge whether the purity meets the requirement for each calculation, and if not, the calculation was repeated. Therefore, the design variables included the total stage of T1 and T2 (N_T and N_{T2}, respectively), the feed stage and recycle stream stage (N_F and N_s, respectively), the side take-off stage (N_O), and the flow rate of side take-off (V). The ratios of N_{T2}, N_F, N_s, N_O, to N_T were design variables in the DHSA. All design variables are marked in Figure 12. Table 8 shows the range of design variables using the SA.

The optimization results are shown in Table 9. The optimal TAC obtained by DHSA is 807,072 $/y, which is 13.0, 1.3, and 4.1% lower than that of the SIM, GA, and POSA, respectively. In terms of calculation times, although the GA, PSOA, and DHSA both stop optimization in advance, the DHSA is still less than the others. From Figure 13a, it can be observed that the TOC takes a dominant position and influences the decrease in the TAC, despite a certain degree of increase in the TCC. As shown in Figure 13b, the optimal TAC obtained by

Table 9. Variable Range and Optimization Results of Case 4

item	range	SIM	GA	PSOA	DHSA
N_T	[15, 55]	37	47	52	48
N_F	[2, N_T]	17	27	31	28(0.602)
N_S	[2, N_T]	4	4	5	4(0.082)
N_{T2}	[2, N_T]	12	8	18	11(0.229)
N_O	[N_{T2}, N_T]	31	39	43	41(0.868)
V (kg/h)	[1,800, 3000]	2600	2424	2571	2403
TAC ($/y)		927,343	818,108	841,308	807,072
NAC		700	340	320	183

https://doi.org/10.1021/acsomega.3c02785
ACS Omega 2023, 8, 28487−28498

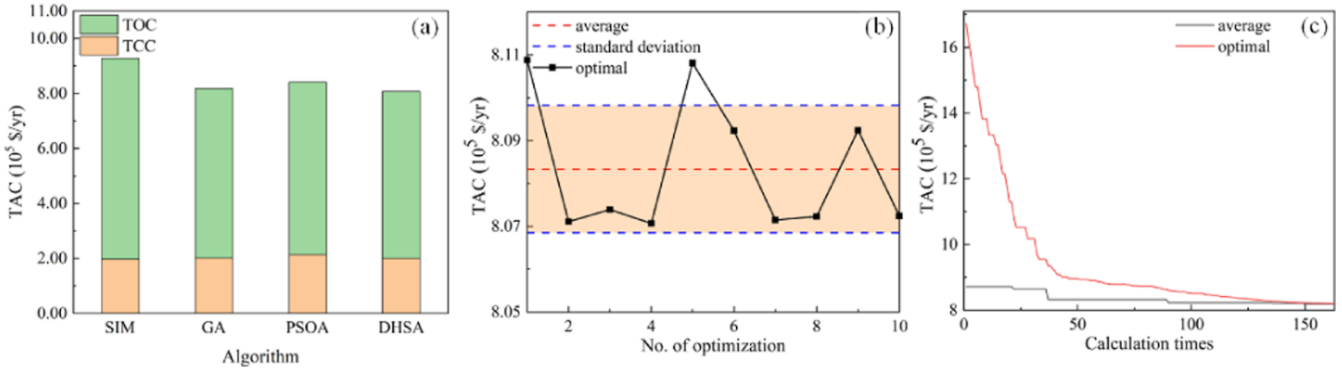

Figure 13. Results of optimization of case 4 TOC and TCC in different algorithms (a); 10 optimization results (b); optimization process (c).

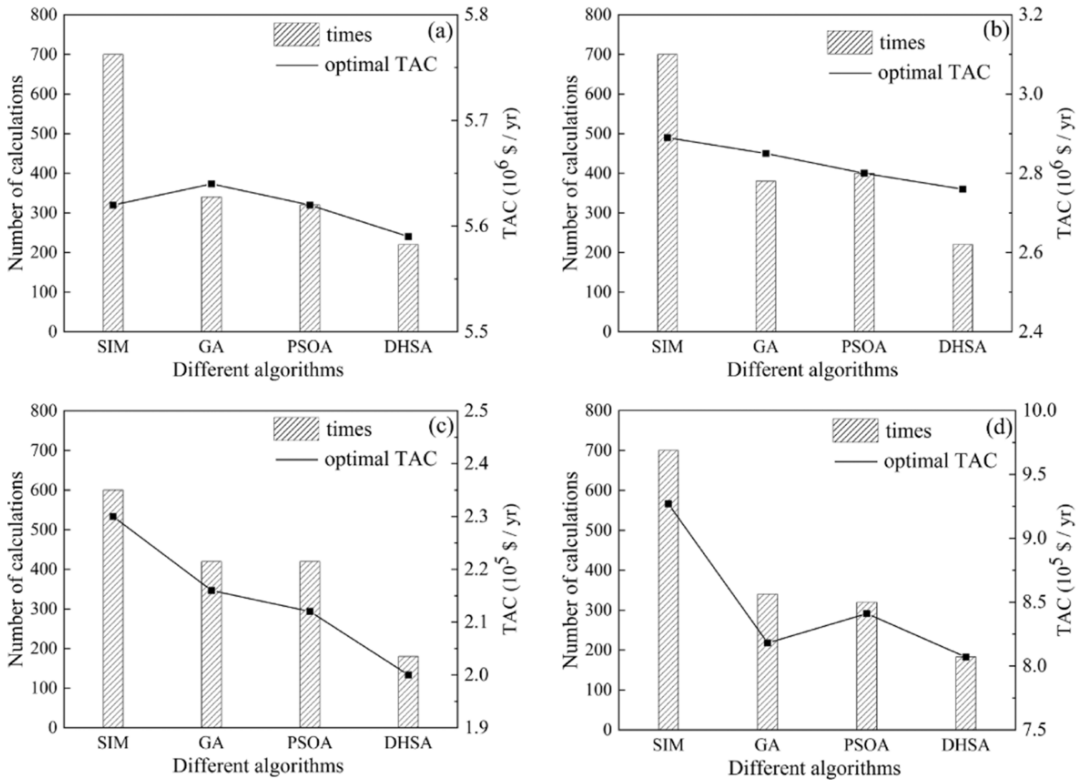

Figure 14. Calculation times and optimal TAC of different algorithms. (a) Case 1, (b) case 2, (c) case 3, and (d) case 4.

repeating the DHSA 10 times is 808,336 $/y on average, and the CV is 0.19%. Figure 13c shows the optimization process corresponding to the optimal solution obtained by DHSA in Table 9. During the optimization process, the optimal value and average value of the HM keep decreasing until the number of calculations reaches 183.

4.5. Discussion. The calculation times and optimal TAC of different algorithms in four distillation optimizations are shown in Figure 14. In case 1, the optimal TACs are close due to the simple characteristics of the two-column model, but calculation times are significantly reduced by using intelligent optimization algorithms, especially the DHSA. In addition, the study of one model has shown that the optimization performance of the DHSA is not as good as the SIM (case 5 in the Supporting Information). Therefore, it is not recommended to use the DHSA for relatively simple processes but rather to obtain the optimal results within an acceptable timeframe through exhaustive search. In other cases, the calculation times and optimal TAC of intelligent optimization algorithms are better than those of the SIM, indicating the advantages of intelligent optimization algorithms in distillation process optimization tasks. Furthermore, among three intelligent optimization algorithms, the DHSA performs the best in terms of optimal TAC and calculation times.

From Figures 7a, 9a, 11a, and 13a, it can be observed that the proportions of TOC and TCC are not consistent. The variation in impact on results can be attributed to the varying degrees of influence exhibited by different variables. As depicted in Figures S2−S5, variables with lower CV exert a more pronounced effect on the results. There are instances where a simultaneous reduction of both factors is possible, while in other cases, achieving optimal results necessitates sacrificing one factor with minimal influence. The conflicting relationship between them makes the distillation process optimization extremely challenging. As the complexity of the process increases, this phenomenon intensifies. In the above

https://doi.org/10.1021/acsomega.3c02785
ACS Omega 2023, 8, 28487−28498

example, the DHSA can obtain satisfactory results, indicating its wide applicability without being affected by variables. Ten parallel optimizations were used to evaluate the stability of the algorithm. Almost all optimal TACs are within a standard deviation as shown in the orange region of Figures 7b, 9b, 11b, and 13b, which indicates that the DHSA can obtain the stable optimal solution all the time and the solution is the global optimal solution in the large probability. The CV of the DHSA in four cases is at a low level and similar (0.17, 0.19, 1.25, and 0.19%, respectively) which not only implies that the results are stable in the same model but also indicates that the error in DHSA is not affected by different models. Tables S1, S2, S4, S5, S7, S8, S10, and S11 show the CV of GA and PSOA in different models, in which the CV is about 10 times that of the DHSA. Therefore, the DHSA has outstanding stability which can search the global optimal TAC in most cases without being affected by the initial population (HM) and the complexity of the model. Figures 7c, 9c, 11c, and 13c show the optimization process of the DHSA in different cases. Both of them exhibit a similar trend, which involves a decrease in the average value (represented by the red line) during the initial stages of optimization, while the optimal value remains unchanged. This is attributed to the strong global search capability brought by the smaller HMCR. As the optimization progresses, the values of HMCR and PAR gradually increase, indicating a shift toward more focused exploration in the vicinity of the optimal value. Consequently, the optimal value starts to decrease significantly (represented by the black line). The optimization process demonstrates the feasibility of dynamically changing HMCR and PAR values in distillation optimization.

5. CONCLUSIONS

A DHSA based on an HSA was first proposed and applied in distillation process optimization in this paper. The improvements of the DHSA include the self-adaptive adjustment of the HMCR, PAR, and BW, the roulette wheel selection strategy based on a mapping between the TAC and fitness, and the replacement of the feed stage and the stage of the section in the distillation column by the ratio to the total stage.

For the practical issues of the distillation process, the DHSA, SIM, GA, and PSOA were applied to optimize four cases: the two-column model, three-column model, reactive distillation column model, and dividing-wall extractive distillation column model. The results demonstrate that the DHSA is capable of achieving superior results in a shorter time frame. Furthermore, as the complexity of the model increases, this advantage becomes even more pronounced. Moreover, the lower coefficient variation in 10 parallel optimization shows that the DHSA has excellent stability in optimizing the distillation process. Therefore, the development of the DHSA is successful for its advantages of high efficiency and strong stability.

This work enriches the application scope of the HSA through its improvement and serves as a practical auxiliary tool for distillation optimization. It can enhance the efficiency of distillation design and result in more competitive design outcomes. Furthermore, it can support future research on the integration of AI in automated distillation design.

■ ASSOCIATED CONTENT

Supporting Information

The Supporting Information is available free of charge at https://pubs.acs.org/doi/10.1021/acsomega.3c02785.

Main code and results of the DHSA and the results of all the cases (PDF)

■ AUTHOR INFORMATION

Corresponding Author

Chao Hua − *Key Laboratory of Green Process and Engineering, Institute of Process Engineering, Chinese Academy of Sciences, Beijing 100190, China;* orcid.org/0000-0001-9747-4656; Email: huachao@ipe.ac.cn

Authors

Zhe Ding − *Key Laboratory of Green Process and Engineering, Institute of Process Engineering, Chinese Academy of Sciences, Beijing 100190, China; School of Chemical Engineering, University of Chinese Academy of Sciences, Beijing 100049, China*

Haohao Zhang − *Key Laboratory of Green Process and Engineering, Institute of Process Engineering, Chinese Academy of Sciences, Beijing 100190, China; School of Chemical Engineering, University of Chinese Academy of Sciences, Beijing 100049, China*

Hai Li − *Key Laboratory of Green Process and Engineering, Institute of Process Engineering, Chinese Academy of Sciences, Beijing 100190, China*

Jinyi Chen − *Key Laboratory of Green Process and Engineering, Institute of Process Engineering, Chinese Academy of Sciences, Beijing 100190, China*

Ping Lu − *Key Laboratory of Green Process and Engineering, Institute of Process Engineering, Chinese Academy of Sciences, Beijing 100190, China*

Complete contact information is available at: https://pubs.acs.org/10.1021/acsomega.3c02785

Notes

The authors declare no competing financial interest.

■ ACKNOWLEDGMENTS

This work was supported by the National Key Research and Development Program of China (2019YFC1907600), Science and Technology Service Network Program (KFJ-STS-QYZD-2021-21-002), and Key Research and Development Program of Ningxia (2022BFH02007).

■ REFERENCES

(1) Kiss, A. A. Distillation Technology-Still Young and Full of Breakthrough Opportunities. *J. Chem. Technol. Biotechnol.* **2014**, *89*, 479−498.

(2) Su, Y.; Jin, S. M.; Zhang, X. P.; Shen, W. F.; Eden, M. R.; Ren, J. Z. Stakeholder-Oriented Multi-Objective Process Optimization Based on an Improved Genetic Algorithm. *Comput. Chem. Eng.* **2020**, *132*, 106618.

(3) Silva, H. G.; Salcedo, R. R. Simop: Application to Global MINLP Stochastic Optimization. *Chem. Eng. Sci.* **2011**, *66*, 1306−1321.

(4) Zhang, H.; Lu, P.; Ding, Z.; Li, Y.; Li, H.; Hua, C.; Wu, Z. Design Optimization and Control of Dividing Wall Column for Purification of Trichlorosilane. *Chem. Eng. Sci.* **2022**, *257*, 117716.

(5) Hosgor, E.; Kucuk, T.; Oksal, I. N.; Kaymak, D. B. Design and Control of Distillation Processes for Methanol-Chloroform Separation. *Comput. Chem. Eng.* **2014**, *67*, 166−177.

(6) Geng, Z. F.; Zhang, K.; Yang, Y. Z.; Gong, H.; Zhang, M. H. Methyl Acetate Hydrolysis Reaction Intensified by Extractive Distillation in Dividing Wall Column. *Chem. Eng. Process.* **2022**, *178*, 109039.

(7) Kirkpatrick, S.; Gelatt, C. D.; Vecchi, M. P. Optimization by Simulated Annealing. *Science* **1983**, *220*, 671−680.
(8) Cheng, J.-K.; Lee, H.-Y.; Huang, H.-P.; Yu, C.-C. Optimal Steady-State Design of Reactive Distillation Processes Using Simulated Annealing. *J. Taiwan Inst. Chem. Eng.* **2009**, *40*, 188−196.
(9) Wang, Y.; Bu, G.; Wang, Y.; Zhao, T.; Zhang, Z.; Zhu, Z. Application of a Simulated Annealing Algorithm to Design and Optimize a Pressure-Swing Distillation Process. *Comput. Chem. Eng.* **2016**, *95*, 97−107.
(10) Cui, Y.; Zhang, Z.; Shi, X.; Guang, C.; Gao, J. Triple-Column Side-Stream Extractive Distillation Optimization via Simulated Annealing for the Benzene/Isopropanol/Water Separation. *Sep. Purif. Technol.* **2020**, *236*, 116303.
(11) Zhu, X. Y.; Zhao, X. X.; Zhang, Z. S.; Ma, Z.; Gao, J. Optimal Design and Control of an Energy-Efficient Triple-Side-Stream Quaternary Extractive Distillation Process. *Chem. Eng. Process.* **2021**, *167*, 108510.
(12) Deb, K.; Pratap, A.; Agarwal, S.; Meyarivan, T. A Fast and Elitist Multiobjective Genetic Algorithm: NSGA-II. *IEEE Trans. Evol. Comput.* **2002**, *6*, 182−197.
(13) Low, K. H.; Sorensen, E. Simultaneous Optimal Design and Operation of Multipurpose Batch Distillation Columns. *Chem. Eng. Process.* **2004**, *43*, 273−289.
(14) Wang, X.-H.; Ding, X.; Du, P.; Tian, Z.-H.; Chen, J.-X. Optimization of a New Integrated Separation Process for Azeotropes Based on Genetic Programming. *Chem. Eng. Technol.* **2021**, *44*, 2355−2364.
(15) He, Q. T.; Li, Q.; Tan, Y. F.; Dong, L. C.; Feng, Z. M. Multi-Objective Optimization of Sustainable Extractive Dividing-Wall Column Process for Separating Methanol and Trimethoxysilane Azeotrope Mixture. *Chem. Eng. Process.* **2022**, *181*, 109141.
(16) Trelea, I. C. The Particle Swarm Optimization Algorithm: Convergence Analysis and Parameter Selection. *Inf. Process. Lett.* **2003**, *85*, 317−325.
(17) Xing, Q.; Kejin, H.; Haisheng, C.; Yang, Y.; Liang, Z. Synthesis and Design of Dividing-Wall Distillation Column Based on Particle Swarm Optimization. *Chem. Ind. Eng. Prog.* **2021**, *40*, 5967−5972.
(18) Babaie, O.; Nasr Esfahany, M. Optimization of a New Combined Approach to Reduce Energy Consumption in the Hybrid Reactive Distillation-Pervaporation Process. *Chem. Eng. Process.* **2020**, *151*, 107910.
(19) Geem, Z. W.; Kim, J. H.; Loganathan, G. v. A New Heuristic Optimization Algorithm: Harmony Search. *Simulation* **2001**, *76*, 60−68.
(20) Yaseen, Z. M.; Aldlemy, M. S.; Oukati Sadegh, M. Non-Gradient Probabilistic Gaussian Global-Best Harmony Search Optimization for First-Order Reliability Method. *Eng. Comput.* **2020**, *36*, 1189−1200.
(21) Mahalingam, S. K.; Nagarajan, L.; Salunkhe, S.; Nasr, E. A.; Davim, J. P.; Hussein, H. M. A. Harmony Search Algorithm for Minimizing Assembly Variation in Non-Linear Assembly. *Appl. Sci.* **2021**, *11*, 9213.
(22) Kaveh, A.; Hosseini, S. M. Improved Bat Algorithm Based on Doppler Effect for Optimal Design of Special Truss Structures. *J. Comput. Civ. Eng.* **2022**, *36* (6), No. 04022028.
(23) Song, Y.; Pan, Q.-K.; Gao, L.; Zhang, B. Improved Non-Maximum Suppression for Object Detection Using Harmony Search Algorithm. *Appl. Soft Comput.* **2019**, *81*, 105478.
(24) Vasebi, A.; Fesanghary, M.; Bathaee, S. M. T. Combined Heat and Power Economic Dispatch by Harmony Search Algorithm. *Int. J. Elec. Power* **2007**, *29*, 713−719.
(25) Yingbo, W.; Lin, W.; Yang, L.; Hua, W. Improved Genetic Harmony Algorithm and Application in Vehicle Routing. *Comput. Meas. Control* **2011**, *19*, 3068−3071.
(26) Mistarihi, M. Z.; Okour, R. A.; Magableh, G. M.; Bany Salameh, H. Integrating Advanced Harmony Search with Fuzzy Logic for Solving Buffer Allocation Problems. *Arabian J. Sci. Eng.* **2020**, *45*, 3233−3244.
(27) Atta, S.; Sinha Mahapatra, P. R.; Mukhopadhyay, A. Solving Tool Indexing Problem Using Harmony Search Algorithm with Harmony Refinement. *Soft. Comput.* **2019**, *23*, 7407−7423.
(28) Kumar, V.; Chhabra, J. K.; Kumar, D. Parameter Adaptive Harmony Search Algorithm for Unimodal and Multimodal Optimization Problems. *J. Comput. Sci.* **2014**, *5*, 144−155.
(29) Ouyang, H.; Gao, L.; Li, S.; Kong, X.; Wang, Q.; Zou, D. Improved Harmony Search Algorithm: LHS. *Appl. Soft Comput.* **2017**, *53*, 133−167.
(30) Keshtegar, B.; Etedali, S. Nonlinear Mathematical Modeling and Optimum Design of Tuned Mass Dampers Using Adaptive Dynamic Harmony Search Algorithm. *Struct. Control Health Monit.* **2018**, *25*, No. e2163.
(31) Hasanipanah, M.; Keshtegar, B.; Thai, D.-K.; Troung, N.-T. An ANN-Adaptive Dynamical Harmony Search Algorithm to Approximate the Flyrock Resulting from Blasting. *Eng. Comput.* **2022**, *38*, 1257−1269.
(32) Jaberipour, M.; Khorram, E. Two Improved Harmony Search Algorithms for Solving Engineering Optimization Problems. *Commun. Nonlinear Sci. Numer. Simul.* **2010**, *15*, 3316−3331.
(33) Guo, Z.; Yang, H.; Wang, S.; Zhou, C.; Liu, X. Adaptive Harmony Search with Best-Based Search Strategy. *Soft Comput.* **2018**, *22*, 1335−1349.
(34) Chakraborty, P.; Roy, G. G.; Das, S.; Jain, D.; Abraham, A. An Improved Harmony Search Algorithm with Differential Mutation Operator. *Fundam. Inf.* **2009**, *95*, 401−426.
(35) Sun, L. Y. *Chemical Engineering Process Simulation Using Aspen Plus*; Chemical Industry Press Co.,Ltd., 2012.
(36) Wang, H. H.; Wang, Z. B.; Zhou, Q.; Liang, J.; Yin, Y.; Su, W. Y.; Wang, G. Y. Optimization and Sliding Mode Control of Dividing-Wall Column. *Ind. Eng. Chem. Res.* **2020**, *59*, 20102−20111.
(37) Sulgan, B.; Furda, P.; Labovska, Z. Effect of Side Reactions in Hybrid Distillation System: Parallel Production of Ethyl Acetate and Glycols. *Chem. Eng. J.* **2022**, *450*, 138154.
(38) Luyben, W. L. Comparison of Extractive Distillation and Pressure-Swing Distillation for Acetone-Methanol Separation. *Ind. Eng. Chem. Res.* **2008**, *47*, 2696−2707.
(39) Yin, M.; Hua, C.; Lu, P.; Zhang, H.; Bai, F. Design and Control of Pressure-Swing Heat Integration Distillation for the Trichlorosilane Purification Process. *ACS Omega* **2022**, *7*, 9254−9266.
(40) Huang, K.; Chen, H.; Zhang, L.; Wang, S.; Liu, W. Effective Arrangement of an External Recycle in Reactive Distillation Columns. *Ind. Eng. Chem. Res.* **2014**, *53*, 1986−1998.
(41) Tian, P. *Optimization And Control of Separating Acetonitrilr/N-Propanol Azeotropic System Using Special Distillation*; Qingdao University of Science and Technology, 2016.

https://doi.org/10.1021/acsomega.3c02785
ACS Omega 2023, 8, 28487−28498